

Molecular docking and 3D-QSAR on 2-(oxalylamino) benzoic acid and its analogues as protein tyrosine phosphatase 1B inhibitors

Mei Zhou and Mingjuan Ji*

*College of Chemistry and Chemical Engineering, Graduate University of Chinese Academy of Sciences,
PO Box 4588, Beijing 100049, PR China*

Received 9 June 2005; revised 24 August 2005; accepted 26 August 2005
Available online 17 October 2005

Abstract—In this paper, molecular docking technique was used to investigate the binding conformation of twelve 2-(oxalylamino) benzoic acid (OBA) inhibitors in the active site of PTP1B. The predicted binding affinities are linearly correlated to the experimental values ($r^2 = 0.859$). Furthermore, comparative molecular field analysis (CoMFA) was conducted based on the binding conformation predicted by molecular docking. The predicted CoMFA model has satisfactory statistical significance and good actual predicted power. The information from molecular docking and CoMFA may give us some valuable hints to the optimization of lead compounds.

© 2005 Elsevier Ltd. All rights reserved.

Protein tyrosine phosphatases (PTPs) are enzymes that can catalyze the removal of phosphate groups from phosphotyrosyl residue in proteins. In conjunction with protein tyrosine kinases (PTKs), they are responsible for the regulation of a wide variety of important cellular processes, such as T-cell activations, cell growth and proliferation, and oncogenic activation.^{1,2} PTP1B, the first purified PTP,³ is an intracellular non-receptor PTPs. It plays a major role in the dephosphorylation of insulin receptor in many cellular and biochemical studies.⁴ A study with PTP1B knockout mice⁵ has demonstrated that loss of PTP1B activity resulted in an enhancement of insulin sensitivity and resistance to weight gain, so potent PTP1B inhibitors may be potential pharmacological agents for the treatment of non-insulin-dependent diabetes mellitus (type 2 diabetes) and obesity. 2-(Oxalylamino) benzoic acid (OBA) has been identified as a general inhibitor of PTPs.⁶ Because of its low molecular weight and enzyme kinetic behavior as a classical and time-independent competitive inhibitor, it has been used as a starting point for structure-based lead optimization to develop selective small molecule inhibitors of PTP1B.⁷

Currently, the binding mode between twelve OBA analogues and PTP1B is systemically analyzed using the flexible docking protocol FlexX. Then, 3D quantitative structure–activity relationship (3D-QSAR) model is developed for 39 OBA inhibitors using the comparative molecular field analyses (CoMFA).^{8,9} We expect that the information obtained from receptor-based method and ligand-based method can validate each other, and afford us effective information for the optimization of the lead compound.

The structure of OBA (compound **1A**) and its analogues and their negative logarithm of dissociate constant K_i values (pK_i obsd) are listed in [Tables 1 and 2](#). The pK_i obsd is used as dependent variables in the FlexX and CoMFA analysis. Of the 39 molecules, 33 were chosen to form a training set to get CoMFA model, and the other six compounds with their names marked with * were chosen as a test set to validate the actual predicting power of the CoMFA model. Computation methods are detailed in [Ref. 10](#).

The total scores (**1A–L**) predicted by FlexX are listed in [Table 1](#). Good correlation ($r^2 = 0.859$, $SD = 0.292$, and $F = 61.0$) between the total score and binding affinity can be observed, which demonstrates that FlexX can quantitatively predict the relative activities of these inhibitors. Besides, we compared **1J** with the ligand in crystal **1C85**.⁶ As shown in [Figure 1](#), the alignment of

Keywords: Protein tyrosine phosphatase; Molecular docking; 3D-QSAR; CoMFA.

* Corresponding author. Tel.: +86 10 88256326; fax: +86 10 88256093; e-mail: jmji@gucas.ac.cn

Table 1. Structure and activity data of inhibitors for CoMFA and FlexX

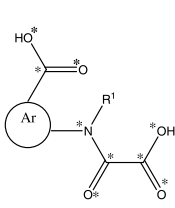
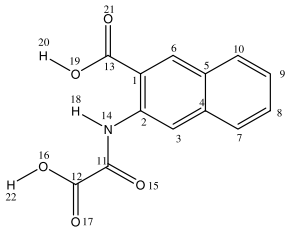
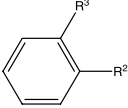
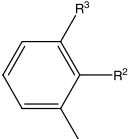
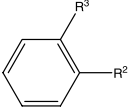
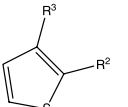
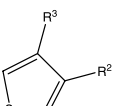
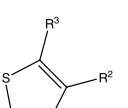
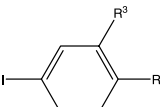
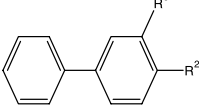
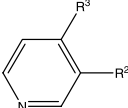
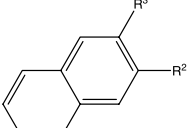
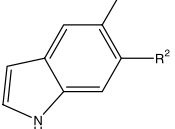
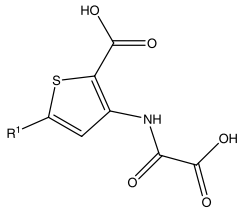
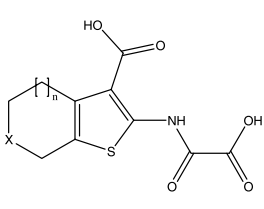
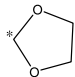
<div style="display: flex; justify-content: space-around; align-items: center;"> <div style="text-align: center;">  <p>1A~1L</p> </div> <div style="text-align: center;">  <p>1J</p> </div> </div>						
Compound	Ar ^a	R ¹	pK _i ^b (obsd)	pK _i (calcd)	Residue	Total score (kJ mol ⁻¹)
1A		H	4.638	3.720	0.919	−154.03
1B		H	2.959	3.045	−0.086	−126.82
1C		Me	2.959	3.017	−0.058	−118.13
1D		H	3.966	3.959	0.007	−128.40
1E*		H	4.124	3.969	0.155	−147.97
1F		H	4.432	3.959	0.473	−147.47
1G		H	4.854	4.997	−0.143	−158.67
1H		H	4.854	5.093	−0.239	−149.52
1I		H	3.796	3.721	0.075	−142.66
1J		H	5.004	5.047	−0.043	−167.07
1K*		H	5.097	4.811	0.286	−162.14

Table 1 (continued)

Compound	Ar ^a	R ¹	pK _i ^b (obsd)	pK _i (calcd)	Residue	Total score (kJ mol ⁻¹)
1L		H	4.745	4.583	0.162	-155.16
1M		H	2.769	3.666	-0.897	
1N		H	2.699	2.909	-0.210	

^a R²=OC(=O)C(=O)NH, R³=COOH.^b K_i (μM) values are measured at pH = 5.5.

Table 2. Structure and activity data of inhibitors for CoMFA

										
2A~2O					3A~3J					
Compound	R ¹	p <i>K</i> _i (obsd)	p <i>K</i> _i (calcd)	Residue	Compound	X	<i>n</i>	p <i>K</i> _i (obsd)	p <i>K</i> _i (calcd)	Residue
2A	Ph	4.886	5.003	−0.117	3A	CH ₂	0	4.921	4.707	0.214
2B	3-Thienyl	4.959	5.097	−0.138	3B	CH ₂	1	5.091	5.257	−0.166
2C	4-(<i>i</i> -Bu)-Ph	4.886	5.052	−0.166	3C*	CH ₂	2	4.921	4.824	0.097
2D	4-F-Ph	5.097	5.078	0.019	3D	O	1	4.854	4.913	−0.059
2E*	4-Cl-Ph	5.000	5.077	−0.077	3E	S	1	5.081	5.100	−0.019
2F	4-HO-Ph	5.347	5.117	0.230	3F	SO	1	5.292	5.170	0.122
2G	4-MeO-Ph	5.046	5.166	−0.120	3G	SO ₂	1	5.215	5.430	−0.215
2H	4-PhO-Ph	4.585	4.612	−0.027	3H	C=O	1	5.886	5.601	0.285
2I	4-BnO-Ph	4.796	4.724	0.072	3I*	CH–OH	1	5.699	5.464	0.235
2J	4-(HOOCCH ₂ -O)-Ph	5.602	5.353	0.249	3J		1	5.658	5.656	0.002
2K	3-NO ₂ -Ph	5.328	5.320	0.008						
2L	3-H ₂ N-Ph	5.215	5.299	−0.084						
2M	3-MeO-Ph	4.921	4.951	−0.030						
2N*	3,4-MeO-Ph	4.602	4.815	−0.213						
2O	3,5-MeO-Ph	5.097	4.896	0.201						

1J and **1A** matches each other very well. Thus the binding conformation predicted by FlexX could be used to analyze the binding mode of these inhibitors with PTP1B.

Figure 2 shows the binding interactions of compound **1J** with PTP1B. **1J** has relatively high binding affinity and good structural rigidity. It can be seen that compound **1J** extended deep into the active-site pocket and formed several hydrogen bonds (marked by dashed lines) with key residues in the catalytic site, especially residue Asp181, which is responsible for substrate phosphate binding. The carboxyl of Asp181 forms three hydrogen bonds with H18 and H20 of **1J**. The lengths of these H-

bonds are 2.12, 2.10 and 2.15 Å, respectively. One H atom of Arg221 forms a hydrogen bond with O16 of **1J**, with the length of 3.02 Å. Furthermore, the mercapto residue Cys215 forms a hydrogen bond with O17 of **1J**. The hydrogen bond networks in the catalytic site of PTP1B must play an important role in determining the level of binding affinities for this kind of inhibitors with PTP1B. Moreover, the van der Waals and hydrophobic interactions should have crucial contribution to ligand binding too. The aromatic portion of **1J** is sandwiched between Tyr46 and Phe182. The centroidal distance between the phenyl of Phe182 and naphthyl of **1J** is 5.05 Å, and that between phenyl of Tyr46 and naphthyl of **1J** is 4.74 Å. The three aromatic rings al-

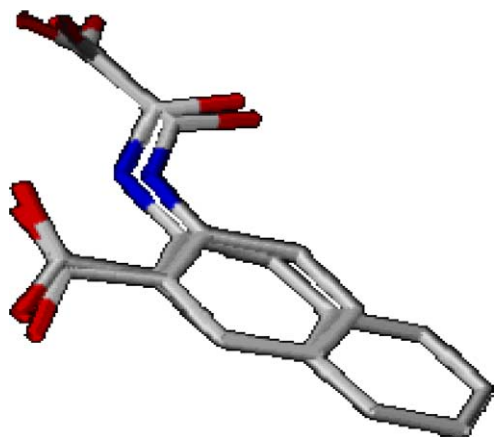


Figure 1. Conformational comparison of compound **1J** from docking and the ligand in crystal **1C85**.

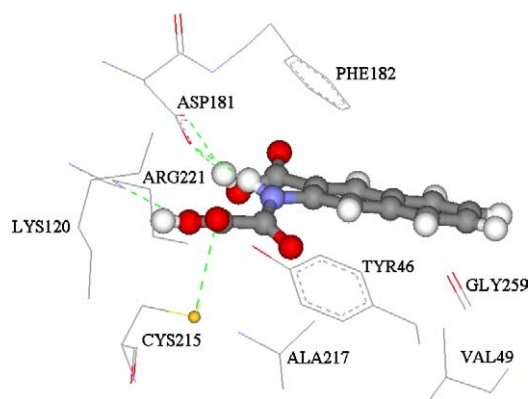


Figure 2. The interactions between **1J** and PTP1B (only important residues of PTP1B directly interacted with **1J** are shown).

most parallel each other, and can form strong π – π stacking interaction.

The CoMFA model obtained from the training set has good statistical significance ($q^2 = 0.650$, $r^2 = 0.880$, $F = 39.872$, and $SD = 0.302$). The linear regression of predicted activity and experimental activity are shown in Figure 3. The predicted binding affinities of six molecules in the test set are within an unsigned mean error as 0.177.

Figure 4A and B shows the contour maps of steric and electrostatic fields, respectively. The steric contour map depicts regions around the molecules where enhanced binding affinity is associated with increasing steric bulk

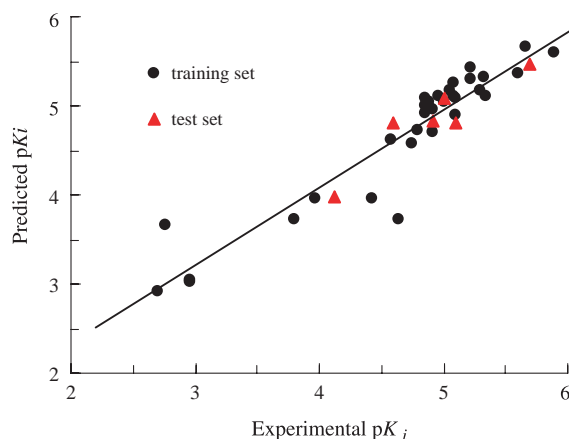


Figure 3. Linear regression of predicted activity and experimental activity for compounds in training set and test set.

in the green area and decreasing steric bulk in the yellow area. The steric contribution to the overall molecular field is 88.7%. Template compound **1J** was treated as the reference molecule. The steric contours shows that around **1J**, there are four sterically unfavorable regions, in which two smaller ones are shown as yellow2 and yellow4 positions, and the other two larger ones are shown as yellow1 and yellow3. Compared with the binding mode predicted by FlexX, we could see that above yellow1 region is the phenyl ring of Phe182, and under the yellow3 and yellow4 region is just the phenyl ring of Tyr46. If large substitutes exist in these regions, the van der Waals interactions and space adoptions may be destroyed. This conclusion is compatible with the binding mode predicted by FlexX, which validates our docking result. By contrast, the green region is on the mouth of the active site, and increasing affinity can be expected when steric bulky groups are introduced into this area. When groups are large enough to interact with residues on the wall of the binding pocket of the receptor, enhancing affinity could be expected by increasing hydrophobic property of the group.

The electrostatic contribution to the overall molecular field is 11.3%. Red regions show negative potential, blue regions show positive potential, and both are favorable for the enhancement of pK_i . While a charge withdrawing or donating group will make the groups linked with it bear more positive or negative charges, blue and red regions are usually neighboring,^{12,13} such as blue2 and red2; they hint at opposite modifying information to the two phenyl rings of the same naphthyl ring. In this

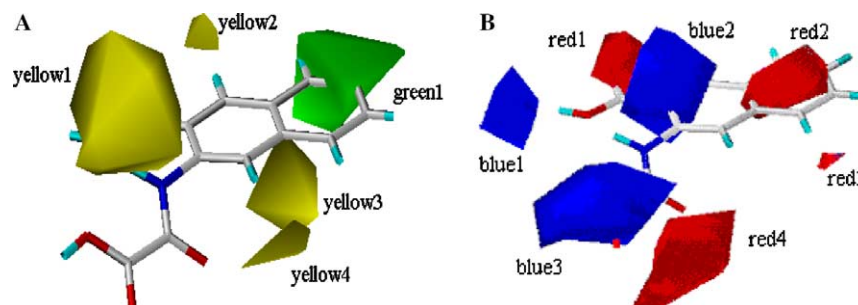


Figure 4. The contour plots of CoMFA steric fields (A) and electrostatic fields (B).

circumstance, distributed range can tell us which kind of electrostatic feature is more important. The blue3 region just covered a carboxyl group (O17–C12–O16–H22) bonding to the aromatic ring through a carbonyl-amino group; this is one of the key structural features of OBA inhibitors. In the binding mode predicted by FlexX, this group can form a H-bond with Cys215. Cys215 is the key residue of PTP1B, so if positive substitutes are introduced here, more binding affinity could be expected. Around the carbonyl group (C11–O15), negative groups are preferred (red4 shows). Another structural feature of OBA inhibitors is the carboxyl group (O21–C13–O19–H20) bound directly to the aromatic group. If negative and positive substitute are imported on the position close to carbonyl and hydroxide radical, respectively, it is favorable for enhancing the affinity.

In the current work, molecular docking simulation shows one potential binding mode of OBA inhibitors with PTP1B. As shown in docking result, the aromatic portion of compound **1J** is sandwiched between Tyr46 and Phe182, and the feature structures of these inhibitors could form several H-bonds with the residues in the active site. Then, CoMFA model validated the binding mode from the view of ligands. The CoMFA contour maps detailed how to improve the binding affinity in three-dimensional space. In addition, in order to get a more native-like binding mode of these inhibitors with PTP1B, the minimization of docking structures and the CoMFA study with the optimized docking alignment is currently underway.

Acknowledgments

The project was supported by the Natural Science Foundation of China (No. 20373089) and Start-up Foundation of Graduate University of Chinese Academy of Sciences (No. M3004).

References and notes

1. Sun, H.; Tonks, N. K. *Trends Biochem. Sci.* **1994**, *19*, 480.
2. Tonks, N. K. *Adv. Pharmacol.* **1996**, *36*, 91.
3. Tonks, N. K.; Diltz, C. D.; Fischer, E. H. *J. Biol. Chem.* **1988**, *263*, 6722.
4. Byon, J. C. H.; Kusari, A. B.; Kusari, J. *Mol. Cell Biochem.* **1998**, *182*, 101.
5. Elchebly, M.; Payette, P.; Michaliszyn, E.; Cromlish, W.; Collins, S.; Loy, A. L.; Normandin, D.; Cheng, A.; Himms-Hagen, J.; Chan, C. C.; Ramachandran, C.; Gresser, M. J.; Tremblay, M. L.; Kennedy, B. P. *Science* **1999**, *283*, 1544.
6. Andersen, H. S.; Iversen, L. F.; Jeppesen, C. B.; Branner, S.; Norris, K.; Rasmussen, H. B.; Møller, K. B.; Møller, N. P. H. *J. Biol. Chem.* **2000**, *275*, 7101.
7. Andersen, H. S.; Olsen, O. H.; Iversen, L. F.; Sørensen, A. L. P.; Mortensen, S. B.; Christensen, M. S.; Branner, S.; Hansen, T. K.; Lau, J. F.; Jeppesen, L.; Moran, E. J.; Su, J.; Bakir, F.; Judge, L.; Shahbaz, M.; Collins, T.; Vo, T.; Newman, M. J.; Ripka, W. C.; Møller, N. P. H. *J. Med. Chem.* **2002**, *45*, 4443.
8. Cramer, R. D.; Patterson, D. E.; Bunce, J. D. *J. Am. Chem. Soc.* **1998**, *110*, 5959.
9. Hou, T.-J.; Xu, X.-J. *Prog. Chem.* **2001**, *13*, 436.
10. All works were done using Sybyl6.7.¹¹ All initial structures were minimized using MMFF94 force field. Molecular docking was performed using FlexX program. The protein used for docking is from Brookhaven Protein Data Bank (PDB code: **1C85**⁶). The original ligand (**1A**) in **1C85** is used as reference structure. Standard parameters of the FlexX program were used. In CoMFA calculations, all OBA derivatives were aligned together with atoms in Table 1 marked with * as their common atoms. Following alignment, the molecules were placed one by one into a 3D cubic lattice with grid 2 Å. The default sp³ carbon atom with +1|e| charge was selected as the probe atom for the calculations of steric and electrostatic fields.
11. Sybyl 6.7; Tripos, Inc.: St. Louis, MO, **1999**.
12. Hou, T.-J.; Li, Z. M.; Li, Z.; Liu, J.; Xu, X.-J. *J. Chem. Inf. Comput. Sci.* **2000**, *40*, 1002.
13. Hou, T.-J.; Zhu, L.-L.; Chen, L.-R.; Xu, X.-J. *J. Chem. Inf. Comput. Sci.* **2003**, *43*, 273.